PHOTONICS Research

Single-mode lasing via loss engineering in fiber-taper-coupled polymer bottle microresonators

Fuming Xie,[1] Ni Yao,[2] Wei Fang,[2] Haifeng Wang,[1] Fuxing Gu,[1,*] and Songlin Zhuang[1]

[1]Shanghai Key Laboratory of Modern Optical Systems, Engineering Research Center of Optical Instrument and System (Ministry of Education), University of Shanghai for Science and Technology, Shanghai 200093, China
[2]State Key Laboratory of Modern Optical Instrumentation, College of Optical Science and Engineering, Zhejiang University, Hangzhou 310027, China
*Corresponding author: fuxinggu@gmail.com

Received 9 June 2017; revised 5 September 2017; accepted 13 September 2017; posted 20 September 2017 (Doc. ID 297652); published 25 October 2017

Due to the lack of mode selection capability, single whispering-gallery-mode (WGM) lasing is a challenge to achieve. In bottle microresonators, the highly nondegenerated WGMs are spatially well-separated along the long-axis direction and provide mode selection according to their axial mode numbers. In this work, we use a loss-engineering approach to suppress the higher-order WGMs and demonstrate single-mode lasing emission in small polymer bottle microresonators. The fiber tapers are not only used to couple pump light into the bottle microresonators to excite the WGMs but also to bring optical losses that are induced from the diameter mismatch between fiber tapers and microresonators. By adjusting the coupling positions, the diameters of fiber tapers, and the coupling angles, single fundamental-mode lasing is efficiently generated with side-mode suppression factors over 15 dB. Our loss-engineering approach is convenient just by moving the fiber taper and may find promising applications in miniature tunable single-mode lasers and sensors.

OCIS codes: (140.3570) Lasers, single-mode; (140.3945) Microcavities; (160.5470) Polymers.

https://doi.org/10.1364/PRJ.5.000B29

1. INTRODUCTION

Whispering gallery mode (WGM) microcavities influence light to circulate for a long time along equatorial trajectories close to the surface before it is scattered or absorbed, thus achieving attractive advantages of long photon lifetime, strong optical field confinement, and in-plane emission, which have been applied to many applications, including lasing, sensing, and optical communications [1–6]. Up to now, various structures have been demonstrated for generating WGM lasers, such as microspheres, microrings, microdroplets, microdisks, microtoroids, and microfibers. Typically, WGM lasers are usually multimode due to the lack of a mode selection strategy [3,6–8]. Reducing the size of the microcavities is a direct way to realize single-mode lasing, and another possible strategy is to use coupled cavities through the Vernier effect [9–11] and the parity-time symmetry effect [12,13].

Recently, bottle microresonators have attracted considerable interest in many applications such as compact optical delay lines, cavity optomechanics, lasing, electromagnetically induced transparency-like phenomenons, and nonlinear optics [14–20]. The highly prolate shapes provide rich spectral features with different intensity distributions along the bottle length, which can be exploited to manipulate resonant modes according to their axial mode numbers and thereby reduce the number of resonances in the spectrum [21,22]. Polymers are good hosts for various lasing gain dopants with advantages of easy processing, mechanical flexibility, and low cost. For example, high-quality polymer microfiber resonators are fabricated to generate WGM lasers, with advantages of tunability, single-mode operation, and enhanced refractive index sensing [11,23]. More recently, we used interference light patterns to spatially overlap the intensity profile of a desired WGM and demonstrated single-mode lasing in polymer bottle microresonators [24]. Attractive advantages, including high side-mode suppression factors (SMSFs) greater than 20 dB, large spectral tunability greater than 8 nm, low lasing threshold, and reversible control, are presented.

Using a fiber taper to couple light into WGM resonators is a common and efficient approach [7,25]. Under critical conditions, high coupling efficiency up to 99% can occur by carefully choosing the diameters of fiber tapers and the gap distance between fiber tapers and resonators [26]. Usually, due to the diameter mismatch between fiber tapers and resonators, although a small portion of input power can be coupled into

resonators, the coupling between fiber tapers and resonators will induce relative large scattering loss. In this work, we use this scattering loss to suppress the higher-order WGMs and demonstrate single-mode lasing emission in small polymer bottle microresonators. When the fiber taper is placed on the side surface of microresonator center, higher-order modes will suffer large optical losses, and only the fundamental mode can be efficiently excited. By carefully adjusting the coupling position and the diameters of the fiber taper, single WGM lasing is demonstrated.

2. EXPERIMENT AND OPERATION PRINCIPLE

In this work, polymer bottle microresonators were fabricated on a silica optical fiber taper using a self-assembled procedure [24]. The gain material Rhodamine 6G (R6G) was dissolved in a trichloromethane solution with a concentration of about 2 wt. %. Epoxy resin (refractive index $n \sim 1.53$) was added to the solvated R6G solution, and the weight ratio of epoxy resin and trichloromethane solution was about (10:2). A microdroplet of R6G-doped epoxy resin solution was picked up using a silica fiber taper with a sharp tip to touch a silica microfiber, which was suspended across a glass channel with a width of ~500 μm [27–29]. Immediately the fiber taper was drawn back. A thin layer of the solution was left on the microfiber, which then rapidly shrank to form a spindle-like shape due to surface tension. Because the droplets' sizes were only several micrometers, gravity force and buoyancy were too small, thus making the surface tension dominate the shape profiles of these droplets. After being solidified by heating at a temperature of 60°C, three parameters were used to estimate each shape of these bottle cavities: bottle outer diameter (D_{out}), fiber taper diameter (D_{fiber}), and neck-to-neck length (L), as denoted in Fig. 1(a). The prolate shape was fitted well with a truncated harmonic oscillator profile. In this work, the bottle microresonators with D_{out} ranging from 3 to 7 μm are investigated.

Benefitting from the supporting optical microfiber, the R6G-doped epoxy resin droplets can be easily and precisely moved and positioned along the microfiber by using a fiber taper probe (before heating the solidification procedure). As shown in Fig. 1(b), the positions of a bottle microresonator can be easily adjusted through a fiber taper probe. In addition, the bottle microresonators can also be merged to obtain a larger size one. As shown in Fig. 1(c), the left one bottle is moved to its adjacent one and the two merge into a single big droplet. By carefully choosing the diameters of microfibers and drawing speed of fiber tapers, many droplets with similar or different shapes can be self-assembled along the silica microfiber. Figure 1(d) shows a picture of several droplets with similar shapes.

To investigate the lasing action in a single bottle microresonator, a silica fiber taper is placed on the bottle microresonator surface to couple pump light into the microresonator. A linear polarized 532 nm pulsed laser (TEM_{00} transverse mode) with a 5 Hz repetition rate and a 10 ns pulse width was used to excite the microresonator. The generated photoluminescence (PL) signals were collected using a long-working distance microscope objective (100×, NA = 0.7) and then were delivered to a spectrometer (iHR 550, JY Horiba Ltd.) for spectral analysis and to a CCD camera (DXM 1200F, Nikon) for image capture. A notch filter (NF01-532U-25, Semrock) was used to block the 532 nm excitation laser when taking CCD images and spectra.

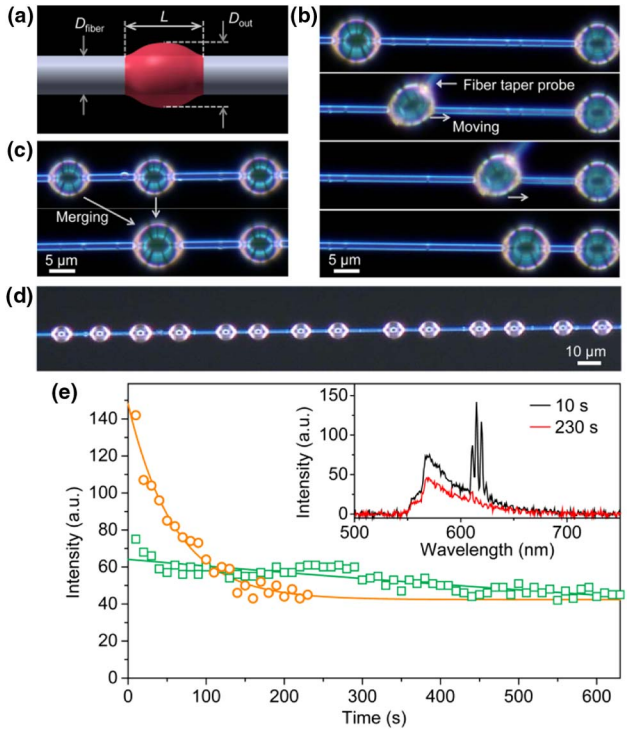

Fig. 1. (a) Definition of D_{out}, D_{fiber}, and L. (b) Moving a microresonator droplet by using a fiber taper probe. (c) Merging two adjacent droplets into a bigger one. (d) Microscope image of many polymer bottle microresonators with similar shapes. (e) PL intensity and lasing intensity correspond to time when exciting a typical R6G-doped bottle microresonator with power around a lasing threshold. Green dots: initial PL intensity. Orange dots: initial lasing intensity.

The photobleaching phenomenon of R6G fluorescent dye depends on the pump laser power. Low excitation power operation is helpful to decrease the photobleaching of fluorescent dye. For pulsed lasers, decreasing repetition rate can also decrease the photobleaching phenomenon. In this work, the repetition rate of a 532 nm laser was greatly decreased as low as 5 Hz in order to minimize the photobleaching phenomenon. Figure 1(e) shows the time-dependent PL intensity and lasing intensity when exciting a typical R6G-doped bottle microresonator with a power around a lasing threshold (about 24.6 nJ), which shows that, after 10 min, over 50% of the initial PL intensity (green dots) still remains, and after 120 s over 50% of the initial lasing intensity (orange dots) at 615 nm still remains.

In bottle microresonators, the highly nondegenerated WGMs are spatially well-separated along the long-axis direction. Under uniform pump, the obtained lasing is usually multimode. When the D_{out} of bottle microresonators decrease (such as less than 8 μm), the free space range (FSR) is comparable or smaller than the width of the optical gain spectrum (~50 nm) [24]. Under this condition, only some transverse modes can be kept within the whole cavity resonance range. As illustrated in Fig. 2(a), the fundamental mode is located at the symmetry center of the bottle cavity, and the higher-order

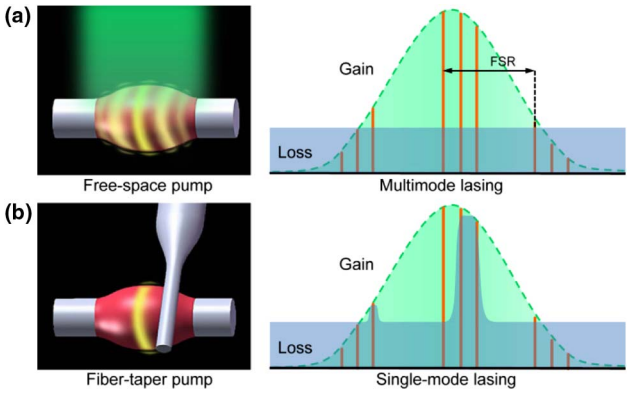

Fig. 2. Principle of single WGM lasing in a polymer bottle microresonator. (a) Multimode lasing behavior under uniform pump. (b) Single WGM lasing by adjusting the coupling position to suppress high-order modes.

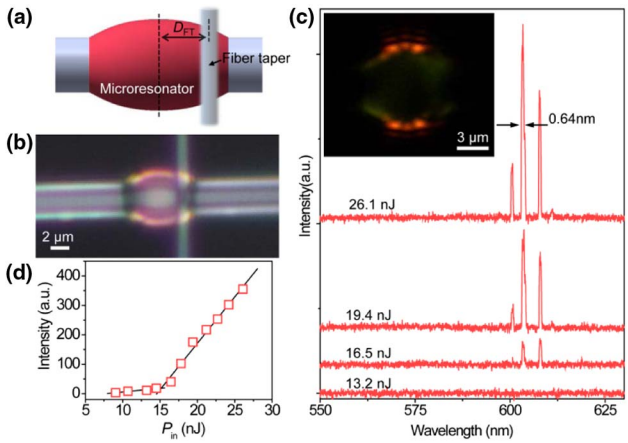

Fig. 3. (a) Illustration of fiber-taper-coupled bottle microresonator. Definition of D_{FT} is denoted. (b) Microscope image of a polymer bottle microresonator ($D_{out} = 5.5$ μm, $D_{fiber} = 3.2$ μm, and $L = 7.5$ μm) coupled with a fiber taper. (c) Emission spectra under fiber-taper-coupled excitation with different pump pulse energy. Inset: dark-field microscope image of the microresonator with $P_{in} = 26.1$ nJ. (d) Emission intensity of the 603.4 nm wavelength peak versus the pump pulse energy.

mode is located on both sides of the center. Here a silica fiber taper is placed on the bottle microresonator surface to couple pump light into the cavity. Under this condition, the coupling position will have a great influence on the resonant mode of the microresonator. Due to the diameter mismatch between the fiber taper and the bottle microresonator, although a small portion of input power can be coupled into the microresonator, the contact between the silica fiber taper, and the microresonator will induce relative large optical loss, including radiation loss, scattering loss, and coupling loss. Thus, when the fiber taper is placed on the side surface of microresonator center, higher-order mode will suffer large loss, and only the fundamental mode can be excited, as shown in Fig. 2(b). It is expected that, by carefully adjusting the coupling position, single WGM lasing can be obtained.

3. RESULTS AND DISCUSSION

The multi-lasing behavior of a fiber taper-coupled R6G-doped bottle microresonator is first investigated. The used R6G-doped bottle microresonator has dimensions of $D_{out} = 5.5$ μm, $D_{fiber} = 3.2$ μm, and $L = 7.5$ μm, as denoted in Fig. 3(a). A fiber taper with a diameter of ~1.2 μm is used to pump the lasing modes. To excite the fundamental mode and higher-order modes, the fiber taper is placed close to the neck of the microresonator at D_{FT} (defined as the distances between the fiber taper with microresonator centerline) of 2.1 μm, with the long-axis direction perpendicular to each other [Fig. 3(b)]. Figure 3(c) presents the lasing spectra versus the pump pulse energy of the 532 nm excitation, in which three narrow dominant peaks sequentially appear as the pump increases. The upper inset in Fig. 3(c) shows an optical microscope image of the microresonator with input pump power (P_{in}) = 26.1 nJ, in which the lasing spots are observed at both top and bottom edges of the bottle microresonator. The measured FWHM is about 0.64 nm at the dominant peak wavelength λ_{peak} of 603.4 nm. Figure 3(d) shows the pumping power-dependent intensities for the $\lambda_{peak} =$ 603.4 nm lasing peaks, in which the measured threshold is 15.3 nJ.

While changing the positions (D_{FT}) of the fiber taper along the axis direction of a bottle microresonator ($D_{out} = 6.1$ μm, $D_{fiber} = 3.9$ μm, and $L = 10.8$ μm), the lasing spectra and their corresponding microscope images were recorded and are shown in Figs. 4(a) and 4(b). For compassion, the lasing spectrum under a uniform free space pump is shown by a black line in Fig. 4(a), which shows that multimode lasing behavior and five typical peaks are denoted. Its corresponding microscope image is shown in Fig. 4(b). When the fiber taper is located on the left side of the microresonator centerline with

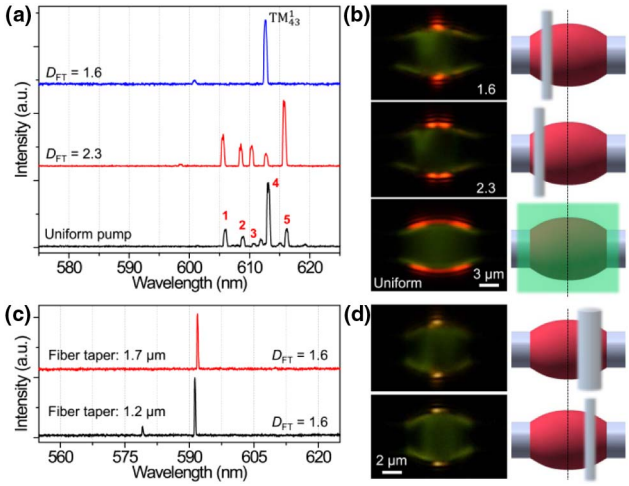

Fig. 4. (a) Lasing spectra and (b) their corresponding microscope images of a polymer bottle microresonator ($D_{out} = 6.1$ μm, $D_{fiber} = 3.9$ μm, and $L = 10.8$ μm) under uniform and fiber taper coupling pump. (c) Lasing spectra and (d) their corresponding microscope images of another polymer bottle microresonator ($D_{out} = 5.3$ μm, $D_{fiber} = 3.9$ μm, and $L = 7.6$ μm) under different diameters of fiber taper coupling pump.

$D_{FT} = 2.3$ μm, five lasing mode emissions are observed. As $D_{FT} = 1.6$ μm, a remarkable lasing peak with $\lambda_{peak} = 612.7$ nm emerges, and also a weak side peak at 600.9 nm is observed. Two single spots at both top and bottom edges are observed in Fig. 4(b). The SMSF is defined as SMSF $= 10 \times \lg[(I_{main} - I_{bg})/(I_{side} - I_{bg})]$, where I_{main} is the dominant lasing mode intensity that subtracts background PL intensity (I_{bg}), and I_{side} is the strongest side-mode intensity that subtracts background PL intensity. Thus, the measured SMSF is about 11.8 dB and the FWHM is about 0.53 nm.

By using a 3D FDTD method [30], we calculate the electromagnetic field distribution in the bottle microresonator. The simulations reveal that the peak of 1 (597.9 nm) corresponds to the transverse-magnetic polarization mode TM^3_{42}, TM^4_{41}, TM^5_{40}, TM^1_{43}, and TM^2_{42}, respectively. Figure 5 shows the electric field intensity distributions of four typical modes on the cross plane of the bottle microresonator along its axis direction. The intensity of TM^1_{43} fundamental mode is concentrated at the centerline, and the intensity of and other bottle modes is distributed symmetrically at both sides of the centerline, with distances of 1.3, 2.3, and 2.6 μm between the two maximum intensity positions, respectively. So by placing a silica fiber taper on the bottle microresonator surface with a proper distance, the higher-order modes can be suppressed.

The diameters of the fiber tapers also affect the side-mode suppression effect. As shown in Fig. 4(c), when a fiber taper with a diameter of 1.2 μm is used to couple a microresonator ($D_{out} = 5.3$ μm, $D_{fiber} = 3.9$ μm, and $L = 7.6$ μm) with $D_{FT} = 1.6$ μm, a 591.3 nm lasing peak is obtained with an SMSF of 8.0 dB. When a fiber taper with a diameter of 1.7 μm is used and maintains the same D_{FT}, the measured SMSF is as high as 15.9 dB. Increase of the SMSF is attributed to the sufficient contraction of the fiber taper on the surface of the microresonator, which induces more optical loss of higher-order WGMs.

The coupling angle (θ_{FT}) between the fiber taper and the long axis of the bottle microresonator can also be adjusted to improve the SMSF. By coupling a fiber taper with a diameter of 1.1 μm to a bottle microresonator ($D_{out} = 5.4$ μm and $L = 8.5$ μm) with their axes perpendicular to each other and with $D_{FT} = 2.1$ μm, as shown in Fig. 6(a), a dominant peak with $\lambda_{peak} = 621.7$ nm and a strong side peak are observed in Fig. 6(b) under $P_{in} = 24.8$ nJ. The measured

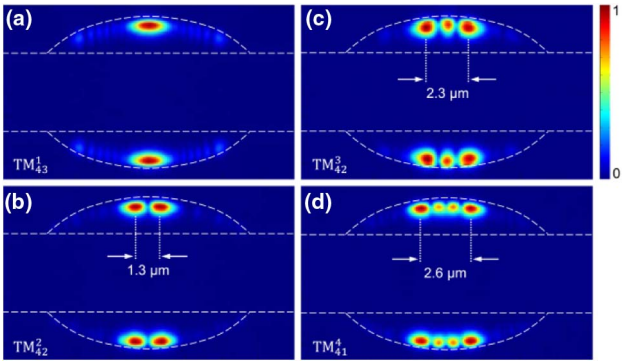

Fig. 5. Electric field-intensity distributions of (a) TM^1_{43}, (b) TM^2_{42}, (c) TM^3_{42}, and (d) TM^4_{41} modes, respectively.

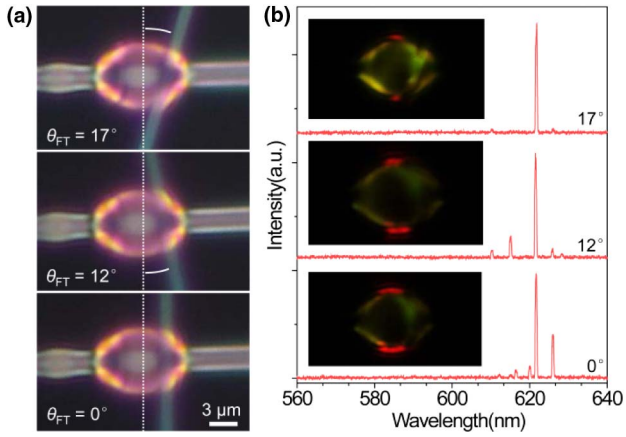

Fig. 6. (a) Lasing spectra and (b) their corresponding microscope images of a polymer bottle microresonator ($D_{out} = 6.1$ μm, $D_{fiber} = 3.9$ μm, and $L = 10.8$ μm) under uniform and fiber taper coupling pump. (c) Lasing spectra and (d) their corresponding microscope images of another polymer bottle microresonator ($D_{out} = 5.3$ μm, $D_{fiber} = 3.9$ μm, and $L = 7.6$ μm) under different diameters of fiber taper coupling pump.

SMSF is about 3.7 dB. When the fiber taper is inclined to the axis of the microresonator with θ_{FT} increasing from 12° to 17°, the intensity of the side peak is dramatically decreased with SMSF increasing from 6.8 to 13.2 dB, respectively. This improvement of the SMSF arises from the enlarged contact area between the fiber taper and the microresonator; thus, higher-order resonant modes suffer greater losses, and the SMSF value is improved.

It is important to point out that the single-mode lasing demonstrated here comes from the small size of the microresonators, but it is not the sole reason because the large FSR of small bottle microresonators can keep only several transverse modes within the whole cavity resonance range by pushing all other modes to the edge or out of the gain range. Our approach is first based on using a large FSR of small bottle microresonators and then is based on using a loss-engineering approach, i.e., these two steps are combined to realize single-mode lasing generation and selection. In addition, the measured thresholds are comparable with most value obtained in WGM microresonators with diameters larger than 10 μm, suggesting that decreasing the dimensions of our bottle microresonators do not increase the lasing threshold. In this work, the bottle microresonators with D_{out} ranging from 3 to 7 μm can well generate single-mode lasing. For microresonators with larger size, there will one over two or three longitudinal modes within the whole cavity resonance range, and their mode intensity will spatially overlap. Thus, it is difficult to generate single-mode lasing as well as single-mode selection.

4. CONCLUSION

In conclusion, we used the loss-engineering approach to suppress the higher-order WGMs and demonstrated single-mode lasing emission in small polymer bottle microresonators. The fiber tapers were not only used to couple pump light into polymer bottle microresonators to excite the resonant WGMs but

also to bring relative large optical loss to them. In small bottle microresonators, the large FSR can keep only several transverse modes within the whole cavity resonance range. By placing the fiber taper on the side surface of microresonator center and carefully adjusting the coupling position, the diameters of the fiber taper, and coupling angles, higher-order WGMs suffer greater losses, and single fundamental mode can be efficiently excited to lase. Our loss-engineering approach to reduce the number of resonances in a spectrum is convenient just by moving the fiber taper and will not damage the microresonators. We believe that our results demonstrated here may find promising applications in miniature tunable single-mode lasers and sensors.

Funding. National Natural Science Foundation of China (NSFC) (11674230); 973 Program (2015CB352001).

Acknowledgment. The authors are grateful for the support provided by the management and technical staff at University of Shanghai for Science and Technology. The authors thank Professor Limin Tong and Dr. Xing Lin at Zhejiang University for their help in numerical calculations and experiments, and Heping Zeng at East China Normal University for helpful discussion.

REFERENCES

1. F. Vollmer and S. Arnold, "Whispering-gallery-mode biosensing: label-free detection down to single molecules," Nat. Methods **5**, 591–596 (2008).
2. A. Chiasera, Y. Dumeige, P. Feron, M. Ferrari, Y. Jestin, G. N. Conti, S. Pelli, S. Soria, and G. C. Righini, "Spherical whispering-gallery-mode microresonators," Laser Photon. Rev. **4**, 457–482 (2010).
3. L. He, S. K. Oezdemir, and L. Yang, "Whispering gallery microcavity lasers," Laser Photon. Rev. **7**, 60–82 (2013).
4. J. Wang, T. Zhan, G. Huang, P. K. Chu, and Y. Mei, "Optical microcavities with tubular geometry: properties and applications," Laser Photon. Rev. **8**, 521–547 (2014).
5. S. Yang, Y. Wang, and H. Sun, "Advances and prospects for whispering gallery mode microcavities," Adv. Opt. Mater. **3**, 1136–1162 (2015).
6. X. F. Jiang, C. L. Zou, L. Wang, Q. H. Gong, and Y. F. Xiao, "Whispering-gallery microcavities with unidirectional laser emission," Laser Photon. Rev. **10**, 40–61 (2016).
7. M. Cai, O. Painter, K. J. Vahala, and P. C. Sercel, "Fiber-coupled microsphere laser," Opt. Lett. **25**, 1430–1432 (2000).
8. V. D. Ta, R. Chen, and H. D. Sun, "Tuning whispering gallery mode lasing from self-assembled polymer droplets," Sci. Rep. **3**, 1362 (2013).
9. L. Shang, L. Y. Liu, and L. Xu, "Single-frequency coupled asymmetric microcavity laser," Opt. Lett. **33**, 1150–1152 (2008).
10. T. Grossmann, T. Wienhold, U. Bog, T. Beck, C. Friedmann, H. Kalt, and T. Mappes, "Polymeric photonic molecule super-mode lasers on silicon," Light Sci. Appl. **2**, e82 (2013).
11. V. D. Ta, R. Chen, and H. Sun, "Coupled polymer microfiber lasers for single mode operation and enhanced refractive index sensing," Adv. Opt. Mater. **2**, 220–225 (2014).
12. L. Chang, X. Jiang, S. Hua, C. Yang, J. Wen, L. Jiang, G. Li, G. Wang, and M. Xiao, "Parity-time symmetry and variable optical isolation in active-passive-coupled microresonators," Nat. Photonics **8**, 524–529 (2014).
13. H. Hodaei, M.-A. Miri, M. Heinrich, D. N. Christodoulides, and M. Khajavikhan, "Parity-time-symmetric microring lasers," Science **346**, 975–978 (2014).
14. M. Sumetsky, "Whispering-gallery-bottle microcavities: the three-dimensional etalon," Opt. Lett. **29**, 8–10 (2004).
15. C. Strelow, H. Rehberg, C. M. Schultz, H. Welsch, C. Heyn, D. Heitmann, and T. Kipp, "Optical microcavities formed by semiconductor microtubes using a bottlelike geometry," Phys. Rev. Lett. **101**, 127403 (2008).
16. M. Poellinger, D. O'shea, F. Warken, and A. Rauschenbeutel, "Ultrahigh-Q tunable whispering-gallery-mode microresonator," Phys. Rev. Lett. **103**, 053901 (2009).
17. M. Sumetsky, "Delay of light in an optical bottle resonator with nanoscale radius variation: dispersionless, broadband, and low loss," Phys. Rev. Lett. **111**, 163901 (2013).
18. K. H. Kim, G. Bahl, W. Lee, J. Liu, M. Tomes, X. Fan, and T. Carmon, "Cavity optomechanics on a microfluidic resonator with water and viscous liquids," Light Sci. Appl. **2**, e110 (2013).
19. Y. Wang, K. Zhang, S. Zhou, Y.-H. Wu, M.-B. Chi, and P. Hao, "Coupled-mode induced transparency in a bottle whispering-gallery-mode resonator," Opt. Lett. **41**, 1825–1828 (2016).
20. Y. Yang, Y. Ooka, R. M. Thompson, J. M. Ward, and S. N. Chormaic, "Degenerate four-wave mixing in a silica hollow bottle-like microresonator," Opt. Lett. **41**, 575–578 (2016).
21. G. S. Murugan, J. S. Wilkinson, and M. N. Zervas, "Selective excitation of whispering gallery modes in a novel bottle microresonator," Opt. Express **17**, 11916–11925 (2009).
22. M. Ding, G. S. Murugan, G. Brambilla, and M. N. Zervas, "Whispering gallery mode selection in optical bottle microresonators," Appl. Phys. Lett. **100**, 081108 (2012).
23. V. D. Ta, R. Chen, L. Ma, Y. J. Ying, and H. D. Sun, "Whispering gallery mode microlasers and refractive index sensing based on single polymer fiber," Laser Photon. Rev. **7**, 133–139 (2013).
24. F. Gu, F. Xie, X. Lin, S. Linghu, W. Fang, H. Zeng, L. Tong, and S. Zhuang, "Single whispering-gallery-mode lasing in polymer bottle microresonators via spatial pump engineering," Light Sci. Appl. **6**, e17061 (2017).
25. J. C. Knight, G. Cheung, F. Jacques, and T. A. Birks, "Phase-matched excitation of whispering-gallery-mode resonances by a fiber taper," Opt. Lett. **22**, 1129–1131 (1997).
26. M. Cai, O. Painter, and K. J. Vahala, "Observation of critical coupling in a fiber taper to a silica-microsphere whispering-gallery mode system," Phys. Rev. Lett. **85**, 74–77 (2000).
27. F. Gu, L. Zhang, Y. Zhu, and H. Zeng, "Free-space coupling of nanoantennas and whispering-gallery microcavities with narrowed linewidth and enhanced sensitivity," Laser Photon. Rev. **9**, 682–688 (2015).
28. F. Liao, G. Wu, and F. Gu, "Hydrogen sensing based on Mach–Zehnder interferometer with palladium-coated microfiber," J. Univ. Shanghai Sci. Technol. **38**, 535–539 (2016).
29. F. Gu, L. Zhang, X. Yin, and L. Tong, "Polymer single-nanowire optical sensors," Nano Lett. **8**, 2757–2761 (2008).
30. X. Lin and W. Fang, "Localized high-Q modes in conical microcavities," Opt. Commun. **381**, 169–173 (2016).